

## *s-p* Hybridization and Electron Shell Structures in Aluminum Clusters: A Photoelectron Spectroscopy Study

Xi Li, Hongbin Wu, Xue-Bin Wang, and Lai-Sheng Wang\*

*Department of Physics, Washington State University, 2710 University Drive, Richland, Washington 99352-1671  
and W. R. Wiley Environmental Molecular Sciences Laboratory, Pacific Northwest National Laboratory, MS K8-88,  
P.O. Box 999, Richland, Washington 99352  
(Received 23 January 1998)*

Using photoelectron spectroscopy of size-selected  $\text{Al}_x^-$  ( $x = 1-162$ ) clusters, we studied the electronic structure evolution of  $\text{Al}_x$  and observed that the Al  $3s$ - and  $3p$ -derived bands evolve and broaden with cluster size and begin to overlap at  $\text{Al}_9$ . Direct spectroscopic signatures were obtained for electron shell structures with spherical shell closings at  $\text{Al}_{11}^-$ ,  $\text{Al}_{13}^-$ ,  $\text{Al}_{19}^-$ ,  $\text{Al}_{23}^-$ ,  $\text{Al}_{35}^-$ ,  $\text{Al}_{37}^-$ ,  $\text{Al}_{46}$ ,  $\text{Al}_{52}$ ,  $\text{Al}_{55}^-$ ,  $\text{Al}_{56}$ ,  $\text{Al}_{66}$ , and  $\text{Al}_{73}^-$ . The electron shell effect diminishes above  $\text{Al}_{75}$  and new spectral features appearing in  $\text{Al}_x^-$  ( $x > 100$ ) suggest a possible geometrical packing effect in large clusters. [S0031-9007(98)06997-X]

PACS numbers: 71.24.+q, 36.40.Cg, 79.60.Bm

The electronic structure of alkali metal clusters can be described well by the jellium model [1–3]. Valence electrons of the metal atoms are delocalized in the volume of the clusters and move in a spherical jellium potential created by the ionic cores. The electrons are quantized according to the spherical orbitals  $|nl\rangle$ , leading to the well-known electron shell structures. Shell structures were first observed in the mass spectra of  $\text{Na}_n$  clusters [1], where particular abundant clusters (magic numbers) were observed at  $n = 8, 20, 40, 58,$  and  $92$ . Trivalent aluminum is a nearly free electron metal [4]. Thus the electronic structure of Al clusters were expected to be described by the jellium model. Figure 1 shows a set of Al clusters (neutrals and anions) which should exhibit shell closings under the spherical jellium model [2]. However, there are two important issues concerning the Al clusters compared to clusters of the monovalent alkali atoms. First, the electronic structure of the Al atom is  $[\text{Ne}]3s^23p^1$  and the energy separation between the  $3s$  and  $3p$  orbitals is about 3.6 eV [5]. For the shell model to hold, one of the  $3s$  electrons has to be promoted to a  $3p$  orbital. This is unlikely in small clusters due to the large  $3p$ - $3s$  energy separation. Therefore, there should exist a critical cluster size range where the separate  $s$  and  $p$  “bands” overlap and the shell model starts to be valid for the larger clusters. Second, the +3 ionic cores of the Al clusters may show larger perturbations to the spherical jellium potential. Thus deviations from the jellium model might be expected at certain cluster sizes. Extensive experimental and theoretical studies have been focused on Al clusters to understand their electronic and structural properties [6–14]. However, there is still no general consensus regarding the above issues. Photoionization experiments suggested a set of shell closings partially consistent with the shell model [8], whereas nonjellium behavior was suggested from static dipole polarizability data [7].

Using photoelectron spectroscopy (PES) of size selected anions, we obtained precise information about the  $s$ - $p$  hybridization and direct spectroscopic signatures

about the electronic shell closings of Al clusters. Previous PES studies of  $\text{Al}_x^-$  were all done with limited cluster sizes or poor energy resolution [9]. No PES data are available above  $\text{Al}_{32}$ , beyond which an extensive set of closed shell clusters is expected (Fig. 1). We have performed an extensive PES study of  $\text{Al}_x^-$  ( $x = 1-162$ ) clusters at 6.42 eV photon energy. Our experiments were performed with an improved magnetic-bottle photoelectron analyzer and a laser vaporization cluster source [15]. Briefly, an aluminum disk target was vaporized at 532 nm (5–10 mJ/pulse) from a Nd:YAG laser. The laser produced plasma was mixed with a He carrier gas pulse at

5s (2) —	330	Al110
4d (10) —	328	
3g (18) —	318	Al106
2i (26) —	300	Al100
1k (34) —	274	Al91
4p (6) —	240	Al80
3f (14) —	234	Al78
2h (22) —	220	Al73
1j (30) —	198	Al66
4s (2) —	168	Al56
3d (10) —	166	Al55
2g (18) —	156	Al52
1i (26) —	138	Al46
3p (6) —	112	Al37
2f (14) —	106	Al35
1h (22) —	92	
3s (2) —	70	Al23
2d (10) —	68	
1g (18) —	58	Al19
2p (6) —	40	Al13
1f (14) —	34	Al11
2s (2) —	20	
1d (10) —	18	
1p (6) —	8	
1s (2) —	2	

FIG. 1. Spherical shell closings and the corresponding closed shell neutral and negative clusters of trivalent Al. The number in the parentheses after each shell index indicates the occupation number,  $2(2l + 1)$ .

a 10 atm backing pressure. A cold cluster beam was produced by a supersonic expansion of the cluster/carrier gas mixture through a 2 mm diam nozzle and collimated by a 6 mm diam skimmer. The anions were extracted from the beam at  $90^\circ$  and mass analyzed by a time-of-flight (TOF) mass spectrometer. The clusters of interest were size selected and decelerated before irradiated by a 193 nm photon beam from an ArF excimer laser. Photoelectron TOF spectra were collected for each size-selected cluster for 10 000 to 30 000 laser shots at 20 Hz repetition rate. The vaporization laser was off at alternating detachment laser shots for background subtraction. For the very small clusters, the anion mass abundance was weak and higher photon flux was needed, causing a more severe noise problem (see Fig. 2). The electron TOF spectra were converted to kinetic energy ( $K_e$ ) spectra calibrated by the known spectra of  $\text{Cu}^-$ . The presented binding energy (BE) spectra were obtained by subtracting the  $K_e$  spectra from the photon energy (6.42 eV). The electron energy resolution of our apparatus was about 30 meV at 1.5 eV  $K_e$  and deteriorates according to  $(K_e)^{3/2}$  for high  $K_e$  (low BE) features.

Figure 2 shows the PES spectra of  $\text{Al}_x^-$  for  $x = 1-12$ . We measured spectra of size-selected  $\text{Al}_x^-$  for  $x = 1$  to 162 systematically. For the very large clusters, the spectra became broad with few changes between spectra of neighboring clusters. The  $\text{Al}^-$  anion has an electron configuration of  $[\text{Ne}]3s^23p^2$ . The peak labeled “ $p$ ” in the spectrum of  $\text{Al}^-$  corresponds to the detachment of a  $3p$  electron, giving rise to the ground state of the Al atom ( $3s^23p^1, ^2P$ ). The peak labeled “ $s$ ” corresponds to the removal of a  $3s$  electron, resulting in an excited Al atom ( $3s^13p^2, ^4P$ ). The measured separation (3.6 eV) between the “ $p$ ” and “ $s$ ” bands agrees with the optical measurement of the  $^2P-^4P$  separation for Al atoms [5]. However, bulk Al is known to have a completely hybridized  $s$ - $p$  band with nearly free electron characters [4]. Thus, we anticipated that the  $p$ - and  $s$ -derived orbitals in small Al clusters would broaden and approach each other, eventually forming a unified  $s$ - $p$  hybridized band at very large sizes.

In small Al clusters, the  $3s$  orbitals of Al form bonding and antibonding molecular orbitals (MOs) which are fully occupied, whereas only the bonding MOs derived from the  $3p$  are partially filled. The PES features from  $p$ - and  $s$ -derived MOs are labeled in Fig. 2 with “ $p$ ” and “ $s$ ”, respectively. The  $s$  features are characterized by their high binding energies and low detachment cross sections. The gap between the  $p$ - and  $s$ -“bands” is seen to be reduced significantly in  $\text{Al}_2$ , and rapidly approaches each other with increasing cluster size. At  $\text{Al}_8$ , the  $p$ - and  $s$ -derived features already begin to overlap partially, and they are completely mixed starting at  $\text{Al}_9$ . Detailed quantum calculations have been performed for the atomic structures of small Al clusters [12,14]. Those with  $n < 6$  were found to be planar. A 2D to 3D structural transition

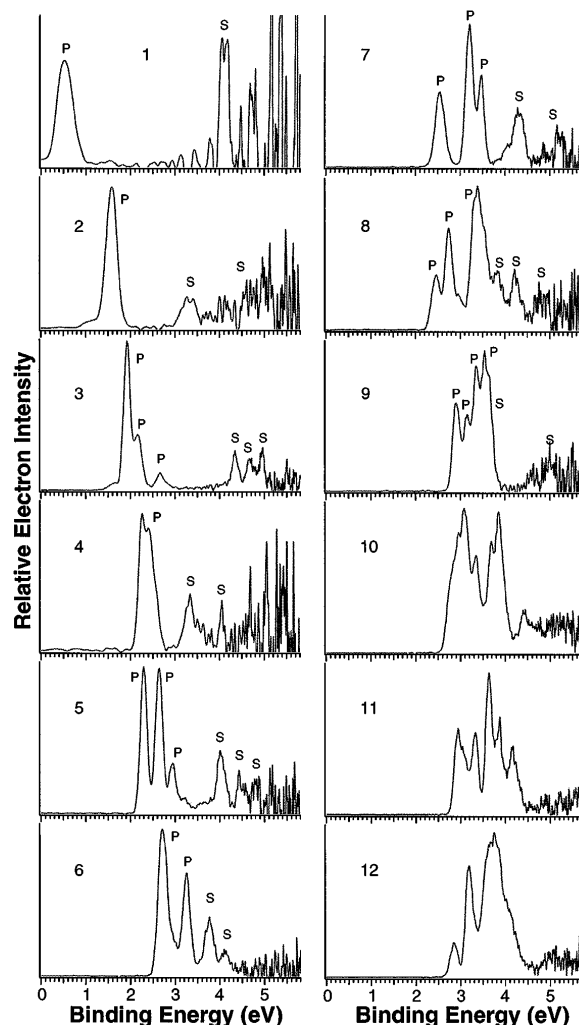


FIG. 2. Photoelectron spectra of  $\text{Al}_x^-$  ( $x = 1-12$ ) at 6.42 eV. The “ $p$ ” and “ $s$ ” labels indicate features derived from the Al  $3p$  and  $3s$ , respectively. Note the overlap of the  $p$ - and  $s$ -derived features in  $\text{Al}_9$ .

occurs between  $\text{Al}_5$  and  $\text{Al}_6$ . The rapid  $s$ - $p$  convergence is accompanied by the structural changes. The complete  $s$ - $p$  mixing starting at  $\text{Al}_9$  is probably due to the high coordination numbers possible for the larger clusters.

According to Fig. 1, the first spherical shell closing occurs at  $\text{Al}_{11}^-$  with the filling of the  $1f$  shell. The PES spectrum of  $\text{Al}_{11}^-$  does show a slightly higher binding energy relative to its neighbors with numerous well-resolved features. However, the shell closing effect in  $\text{Al}_{11}^-$  is not as strong as observed in the larger clusters (Fig. 2), probably because  $\text{Al}_{11}^-$  is still quite small and its electronic structure is likely to be dictated more by its detailed molecular structure. A much stronger shell closing effect was observed at  $\text{Al}_{13}^-$  and larger clusters as shown in Figs. 3 and 4. Figure 3 shows the PES spectra of the closed shell anions (left column) compared to those one atom larger (right column). The closed shell anion clusters ( $\text{Al}_x^-$ ) exhibit high binding energies

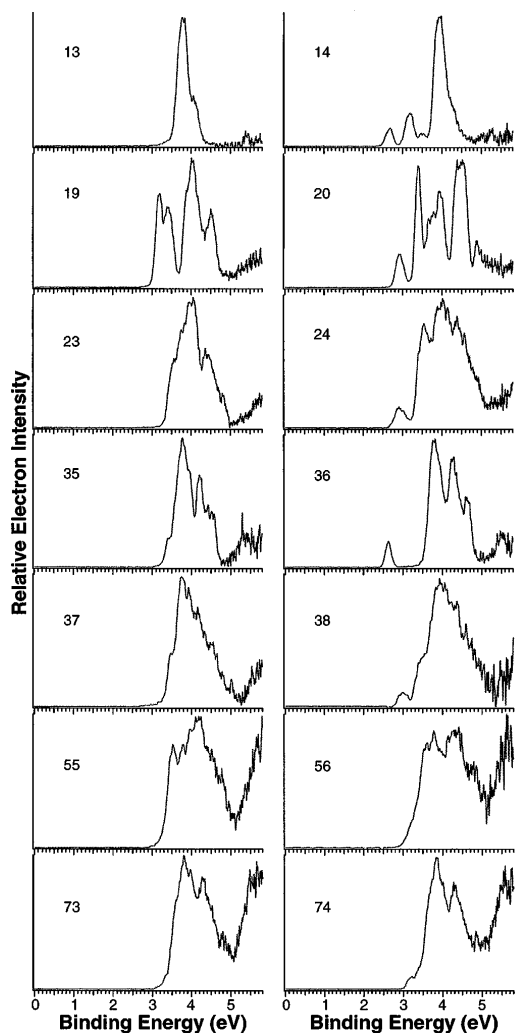


FIG. 3. Photoelectron spectra of the expected closed shell  $Al_x^-$  anions compared to those of the  $Al_{x+1}^-$  clusters. Note the high binding energies of the closed shell  $Al_x^-$  clusters and the appearance of low binding energy features and energy gaps in the  $Al_{x+1}^-$  clusters.

and high degeneracy, whereas those clusters one atom larger ( $Al_{x+1}^-$ ) show weak low energy features with energy gaps, suggesting partial occupation of the next higher shells according to Fig. 1.  $Al_{13}^-$ , with 40 valence electrons, exhibits the strongest shell closing effect. The electron affinity derived for  $Al_{13}$  is 3.62 eV, the highest of all the Al clusters we investigated. The spectrum of  $Al_{13}^-$  shows the fewest features, indicating a high degeneracy and high symmetry, consistent with the known icosahedral geometry ( $I_h$ ) for  $Al_{13}$  [12,13].  $Al_{14}^-$ , with 43 valence electrons, was expected to partially fill the  $1g$  shell, which should undergo ellipsoidal splitting [16]. The spectrum of  $Al_{14}^-$  is almost identical to that of  $Al_{13}^-$  except for the three weak low energy features (Fig. 3) which are consistent with the anticipated splitting of the  $1g$  level. Ellipsoidal distortion in open-shell clusters leads to subshell structures and subshell closings [16]. The

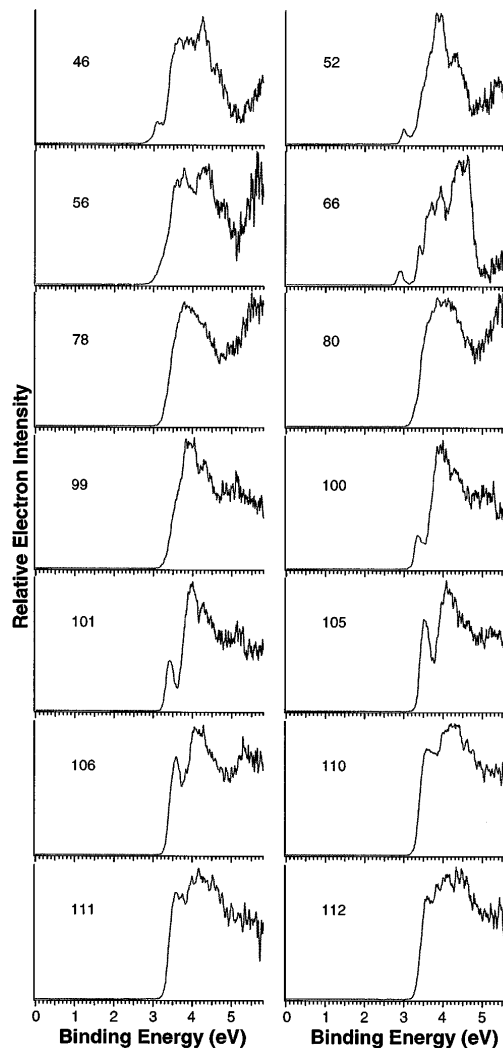


FIG. 4. Photoelectron spectra of  $Al_x^-$  anions for which the corresponding neutrals are expected to be closed shell and those of larger  $Al_x^-$  clusters ( $x = 99-112$ ).

PES spectra of the other  $Al_{x+1}^-$  clusters in Fig. 3 suggest that the neutral  $Al_{x+1}$  clusters are all closed shell with a substantial energy gap. In particular,  $Al_{36}$  exhibits an unusually large energy gap (1.02 eV). The PES spectra of those clusters, for which the neutrals were expected to be closed shell in the spherical shell model (Fig. 1), are shown in Fig. 4 along with those of several large clusters. For  $Al_{46}^-$ ,  $Al_{52}^-$ , and  $Al_{66}^-$ , a weak low energy feature was clearly resolved with a significant energy gap, indicating the neutral clusters are indeed closed shell. For  $Al_{56}^-$  alone, the weak low energy feature was not well resolved and only a shoulder was observed, suggesting a smaller energy gap between the  $4s$  and  $1j$  shells (Fig. 1). We observed additional closed shell neutral clusters,  $Al_{26}$ ,  $Al_{28}$ ,  $Al_{32}$ ,  $Al_{42}$ ,  $Al_{54}$ ,  $Al_{68}$ , and  $Al_{72}$ , probably due to subshell closings.

However, the spectra of  $Al_{78}^-$  and  $Al_{80}^-$  (Fig. 4) do not show a similar energy gap even though the

corresponding neutral clusters were expected to be closed shell (Fig. 1). This could be due to the fact that the ordering of the higher electron shells is different from that shown in Fig. 1, giving a different set of spherical shell closings. However, we did not observe any electronic features resembling shell closings in the clusters larger than  $\text{Al}_{75}^-$ . The PES spectra for the larger clusters showed broad features similar to those of  $\text{Al}_{78}^-$  and  $\text{Al}_{80}^-$  up to  $\text{Al}_{99}^-$  (Fig. 4). Starting at  $\text{Al}_{100}^-$ , a new low energy feature appeared abruptly. The new feature persisted and grew in intensity until  $\text{Al}_{112}^-$  where it merged with the higher energy features. The PES spectra then again became broad and featureless. Instead of suggesting a shell closing at  $\text{Al}_{100}$ , the new PES feature appeared in  $\text{Al}_{100}^-$  and the larger clusters seemed to indicate a geometrical packing effect. The new PES feature may suggest the onset of a new atomic shell and the intensity of this feature increased as the shell was being filled. In fact, octahedral atomic shell packing has been suggested for large aluminum clusters [17]. Clearly, the nature of the spectral transition between  $\text{Al}_{75}^-$  and  $\text{Al}_{100}^-$  and the spectral evolution at larger clusters deserve further investigation.

The observation of electron shell structures starting from about  $\text{Al}_{13}^-$  is consistent with our observation of the  $s$ - $p$  hybridization starting from  $\text{Al}_9$ . All the shell closings observed in our data agree with those assigned from previous photoionization studies [8]. However, more closed shell clusters were observed in our experiments, due to the direct electronic structure signatures of energy gaps evidenced in the PES data. Quantitative understanding of the fine electronic features contained in the PES spectra will no doubt require accurate quantum calculations by taking into account detailed cluster geometrical structures, particularly for the small clusters. However, the shell model does provide a qualitative picture and predict the closed shell clusters well. The evolution of the PES spectra beyond  $\text{Al}_{75}$  and the fact that no shell closings seemed to exist are intriguing. Previous theoretical studies suggested that for  $\text{Al}_{55}$  a face-centered cubic structure was already energetically comparable to an  $I_h$  cluster [13]. It is thus reasonable to assume that for larger clusters lattice based structures may dominate [10,17] and the simple electron shell model is no longer adequate.

Support of this research by the National Science Foundation is gratefully acknowledged. The work was performed at Pacific Northwest National Laboratory, operated for the U.S. Department of Energy by Battelle

under Contract No. DE-AC06-76RLO 1830. L. S. W. acknowledges financial support from the Alfred P. Sloan Foundation.

---

\*Author to whom correspondence should be addressed.

- [1] W. D. Knight *et al.*, Phys. Rev. Lett. **52**, 2141 (1984).
- [2] W. Ekardt, Phys. Rev. B **29**, 1558 (1984); M. L. Cohen *et al.*, J. Phys. Chem. **91**, 3141 (1987).
- [3] W. A. de Heer, Rev. Mod. Phys. **65**, 611 (1993); M. Brack, *ibid.* **65**, 677 (1993).
- [4] N. W. Ashcroft and N. D. Mermin, *Solid State Physics* (Holt, Rinehart, and Winston, New York, 1976).
- [5] C. E. Moore, in *Atomic Energy Levels*, Natl. Bur. Stand. (U.S.) Circ. (U.S. GPO, Washington, D.C., 1971), Vol. I.
- [6] M. F. Jarrold, J. E. Bower, and J. S. Kraus, J. Chem. Phys. **86**, 3876 (1987); D. M. Cox *et al.*, *ibid.* **84**, 4651 (1986); S. A. Ruatta, L. Hanley, and S. L. Anderson, Chem. Phys. Lett. **137**, 5 (1987).
- [7] W. A. de Heer, P. Milani, and A. Chatelain, Phys. Rev. Lett. **63**, 2834 (1989).
- [8] K. E. Schriver *et al.*, Phys. Rev. Lett. **64**, 2539 (1990); J. L. Persson *et al.*, Chem. Phys. Lett. **186**, 215 (1991); M. Pellarin *et al.*, J. Chem. Phys. **98**, 944 (1993).
- [9] K. J. Taylor *et al.*, Chem. Phys. Lett. **152**, 347 (1988); G. Gantefor *et al.*, Faraday Discuss. Chem. Soc. **86**, 197 (1988); G. Gantefor and W. Eberhardt, Chem. Phys. Lett. **217**, 600 (1994); C. Y. Cha, G. Gantefor, and W. Eberhardt, J. Chem. Phys. **100**, 995 (1994).
- [10] B. Bagueard *et al.*, J. Chem. Phys. **100**, 754 (1994).
- [11] E. Cottancin *et al.*, *ibid.* **107**, 757 (1997); J. Lerme *et al.*, Phys. Rev. Lett. **68**, 2818 (1992).
- [12] T. H. Upton, J. Chem. Phys. **86**, 7054 (1987); L. G. M. Pettersson, C. W. Bauschlicher, and T. Halicioglu, *ibid.* **87**, 2205 (1987).
- [13] J. Y. Yi, D. J. Oh, and J. Bernholc, Phys. Rev. Lett. **67**, 1594 (1991); H. P. Cheng, R. S. Berry, and R. L. Whetten, Phys. Rev. B **43**, 10 647 (1991); S. N. Khanna and P. Jena, Phys. Rev. Lett. **69**, 1664 (1992).
- [14] R. O. Jones, Phys. Rev. Lett. **67**, 224 (1991); J. Chem. Phys. **99**, 1194 (1993).
- [15] L. S. Wang, H. S. Cheng, and J. Fan, J. Chem. Phys. **102**, 9480 (1995); L. S. Wang and H. Wu, in *Cluster Materials*, Advances in Metal and Semiconductor Clusters Vol. 4, edited by M. A. Duncan (Jai Press, Greenwich, 1998), pp. 299–343.
- [16] K. Clemenger, Phys. Rev. B **32**, 1359 (1985).
- [17] T. P. Martin, U. Naher, and H. Schaber, Chem. Phys. Lett. **199**, 470 (1992); U. Naher, U. Zimmermann, and T. P. Martin, J. Chem. Phys. **99**, 2256 (1993).